Synthesis and Characterization of New Chiral Side Chain Liquid Crystalline Polyoxetanes

Yong-Kuk Yun,† Doo-Hyun Ko, and Jung-Il Jin*

Department of Chemistry and Center for Electro- and Photo-Responsive Molecules, Korea University, Seoul, 136-701, Korea

Yoon Sok Kang and Wang-Cheol Zin

Department of Materials Science and Engineering, Pohang University, Pohang, 790-784, Korea

Byung-Wook Jo

Department of Chemical Engineering, Chosun University, Kwang-Ju 501-759, Korea

Received February 28, 2000; Revised Manuscript Received May 19, 2000

ABSTRACT: Two series of the side chain liquid crystalline polyoxetanes were synthesized via cationic ring-opening polymerization of oxetane monomers bearing pendant mesogenic units including two chiral carbons. The first two polymers have only one pendant group in the repeating unit, whereas the second polymers have two mesogenic groups per repeating unit. The oxetane monomer bearing one mesogenic unit produced high molecular weight polymers, whereas the ones bearing two mesogenic units at the same carbon in the ring produced only oligomeric products. Thermal and liquid crystalline properties of the polymers were investigated by optical polarizing microscopy, differential scanning calorimetry (DSC), and small- and wide-angle X-ray diffractometry. All of the polymers, with the exception of only one polymer, formed liquid crystalline phases such as S_A, S_C*, and S_I* phases in melts. The molecular arrangement in the smectic phases was interpreted as an intercalated bilayer structure. An attempt to study the ferroelectric properties of the polymers was made, but the results obtained were not satisfactory.

Introduction

Since ferroelectricity of the S_C* phase was reported by Meyer[1] in 1975, numerous ferroelectric liquid crystalline compounds (FLCs) have been synthesized and characterized.[2−6] The FLCs show, in general, fast response times in electric fields; for that reason, they have a potential for electrooptic displays.[2,7−9] In comparison with the FLCs, ferroelectric side-chain liquid crystalline polymers (FSLCPs)[10−18] have shortcomings of higher melt viscosity and, thus, longer switching time. Despite these disadvantages, FSLCPs are still attractive materials because their polymeric nature results in better mechanical strength when compared with those of FLCs.[16,19−22] Furthermore, if the chemical structure of the polymer is properly designed, in other words, if they have a flexible main chain backbone and a sufficient spacer length so that the side group mesogens are efficiently decoupled from the polymer backbone, FSLCPs having fast switching times in the microsecond region can be obtained.[23, 24]

In the case of earlier reports on FSLCPs, the polymer backbones were of mainly poly(meth)acrylates[16−18,25] or polysiloxanes.[14,15,19,22−24] Recently, a few research groups have utilized polyoxetane as a new type of backbone structure.[26−30] Although they reported the synthesis and the liquid crystallinity of some of the side-chain LCPs, systematic study on structure−property relationships of these new FSLCPs is still required. Furthermore, to our knowledge, only one investigation of side chain polyoxetanes exhibiting the chiral smectic C phase was reported by Hsu et al.[31] Surprisingly, their polymers showed relatively fast switching times in the range of microseconds (μs). The chemical structures of their ferroelectric polyoxetanes are shown below.

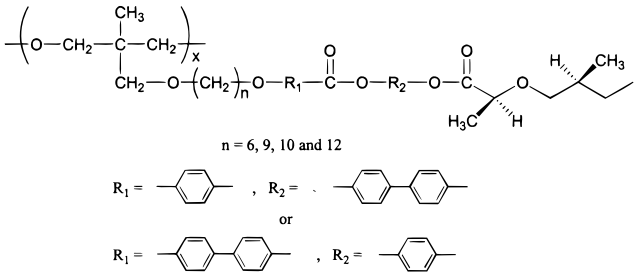

In the present investigation, we prepared two series of new side-chain LC polyoxetanes by cationic ring-opening polymerization of monomers consisting of the oxetane ring, polymethylene flexible spacers and mesogenic units including two chiral carbons. We systematically studied their liquid crystalline properties and molecular orientation in the mesophase by detailed X-ray diffractometry as well as by differential scanning calorimetry (DSC) and optical photomicroscopy. The drawings on the next page show the chemical structures of our side-chain LC polyoxetanes:

Experimental Section

Synthesis of Monomers. 3-[[ω-{4′-(2*S*,3*S*)-2-Chloro-3-methyl-*n*-pentanoyloxy}-4-biphenylalkoxy]methyl]-3-methyloxetanes, 3(*n*), and 3,3′-Bis[[ω-{4′-{(2*S*,3*S*)-2-chloro-3-methyl-*n*-pentanoyloxy}-4-biphenyloxy}alkyloxy]-methyl]oxetanes, 10(*n*). The four monomers, **3(6)**, **3(10) 10-(6)**, and **10(10)**, newly synthesized in this investigation, were prepared following the routes shown in Schemes 1 and 2. The details of the monomer synthesis are available in Supporting Information. Only structural information on the monomers is given below.

† Present address: Department of Materials Science & Engineering, University of Illinois at Urbana-Champaign, 1304 W. Green St. Urbana, IL 61801.

10.1021/ma000346u CCC: $19.00
Published on Web 08/10/2000

Scheme 1. Synthetic Route to Monomers for Polymer-1(*n*)

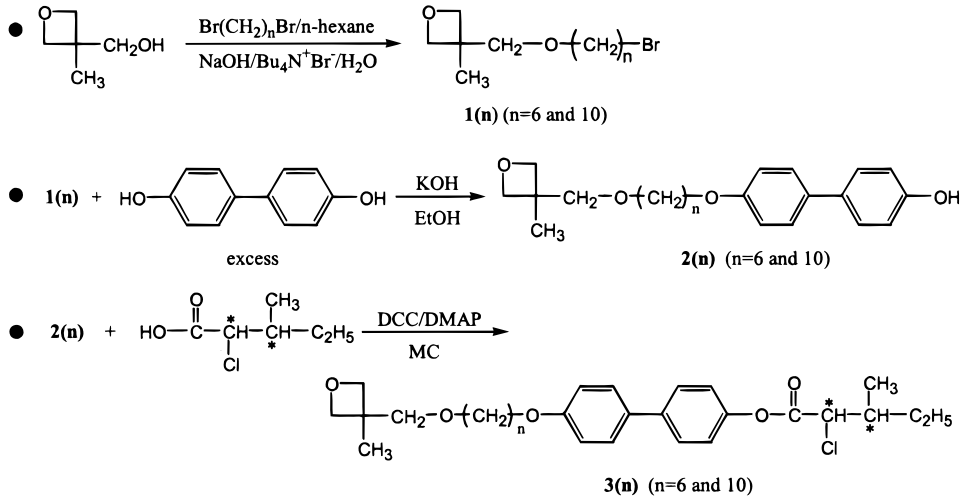

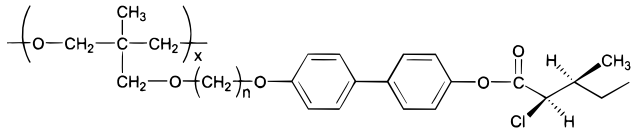

Polymer-1(n) (n = 6 and 10)

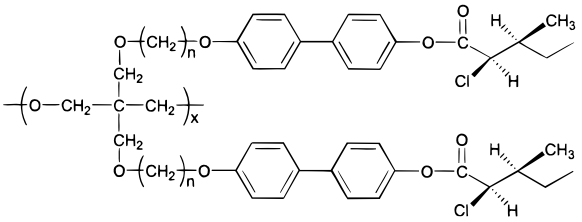

Polymer-2(n) (n = 6 and 10)

3-[[6-{4′-{(2*S*,3*S*)-2-Chloro-3-methyl-*n*-pentanoyloxy}-4-biphenyloxy}hexyloxy]methyl]-3-methyloxetane, 3(6). Mp: 47 °C. IR (KBr): 3041 (aromatic C−H stretching), 2911 and 2799 (aliphatic C−H stretchings), 1762 (C═O stretching), 1608 and 1480 (aromatic C═C stretchings), 1382, 1229, 1167, 1035, and 980 (C−O stretchings), and 520 cm^{-1} (C−Cl stretching). ^1H NMR ($CDCl_3$, ppm): δ 0.95−1.9 (m, 19H, $-CH_2-$ and $-CH_3$), 2.25 (m, 1H, −ClCH−*CH*−), 3.50 (s + t, 4H, oxetane ring−*CH*$_2$−O− and −O−*CH*$_2$−CH$_2$), 4.00 (t, 2H, $-CH_2-$OAr), 4.40 (m, 3H, Cl−CH− and $-CH_2-$ in the oxetane ring), 4.55 (d, 2H, $-CH_2-$ in the oxetane ring), 6.97, 7.20, 7.50, and 7.57 (d, 8H, Ar−H). Anal. Calcd for $C_{29}H_{39}ClO_5$: C, 69.24; H, 7.81; O, 15.90. Found: C, 69.31; H, 7.79; O, 15.92.

3-[[10-{4′-{(2*S*,3*S*)-2-Chloro-3-methyl-*n*-pentanoyloxy}-4-biphenyloxy}decyloxy]methyl]-3-methyloxetane, 3(10). Mp: 41 °C. IR (KBr): 3041 (aromatic C−H stretching), 2908 and 2797 (aliphatic C−H stretchings), 1762 (C═O stretching), 1608 and 1479 (aromatic C═C stretchings), 1378, 1194, 1038, and 980 (C−O stretchings), and 520 cm^{-1} (C−Cl stretching). ^1H NMR ($CDCl_3$, ppm): δ 0.95−1.9 (m, 27H, $-CH_2-$ and $-CH_3$). 2.23 (m, 1H, −ClCH−*CH*−), 3.45 (s + t, 4H, oxetane ring−*CH*$_2$−O− and −O−*CH*$_2$−CH$_2$−), 4.00 (t, 2H, $-CH_2-$OAr), 4.37 (m, 3H, Cl−CH− and $-CH_2-$ in the oxetane ring), 4.50 (d, 2H, $-CH_2-$ in the oxetane ring), 6.96, 7.15, 7.50, and 7.57 (d, 8H, Ar−H). Anal. Calcd for $C_{33}H_{47}ClO_5$: C, 70.88; H, 8.47; O, 14.31. Found: C, 70.80; H, 8.44; O, 14.28.

3,3′-Bis[[6-{4′-{(2*S*, 3*S*)-2-chloro-3-methyl-*n*-pentanoyloxy}-4-biphenyloxy}hexyloxy]methyl]oxetane, 10(6). Mp: 54 °C. IR (KBr): 2935 and 2866 (aliphatic C−H stretchings), 1757 (C═O stretching), 1606 and 1497 (aromatic C═C stretchings), and 1286, 1116, and 977 cm^{-1} (C−O stretchings). ^1H NMR ($CDCl_3$, ppm): δ 0.9−1.8 (m, 32H, $-CH_2-$ and CH_3), 2.2 (m, 2H, −ClCH−*CH*−), 3.5 (m, 4H, −*CH*$_2$−O−CH$_2$− oxetane ring), 3.6 (s, 4H, −O−CH$_2$−oxetane ring), 4.0 (t, 4H, $-CH_2-$ O−Ar), 4.2 (d, 2H, Cl−*CH*−), 4.3 (s, 4H, $-CH_2-$ in the oxetane ring), 6.8, and 6.9 (d, 8H, Ar−H) and 7.4 (m, 8H, Ar−H). Anal. Calcd for $C_{53}H_{68}Cl_2O_9$: C, 69.19; H, 7.45; O, 15.65. Found: C, 69.17; H, 7.50; O, 15.61.

3,3′-Bis[[10-{4′-{(2*S*,3*S*)-2-chloro-3-methyl-*n*-pentanoyloxy}-4-biphenyloxy}decyloxy]methyl]oxetane, 10(10). Mp: 60.5 °C. IR (KBr): 2926 and 2854 (aliphatic C−H stretchings), 1762 (C═O stretching), 1605 and 1497 (aromatic C═C stretchings), and 1213, 1170, and 981 cm^{-1} (C−O stretchings). ^1H NMR ($CDCl_3$, ppm): δ 0.9−1.8 (m, 48H, $-CH_2-$ and CH_3), 2.2 (m, 2H, −ClCH−*CH*−), 3.5 (m, 4H, −*CH*$_2$−O−CH$_2$−oxetane ring), 3.6 (s, 4H, −O−CH$_2$−oxetane ring), 4.0 (t, 4H, $-CH_2-$ O−Ar), 4.4 (d, 2H, Cl−*CH*−), 4.5 (s, 4H, $-CH_2-$ in the oxetane ring), 6.9, and 7.1 (d, 8H, Ar−H) and 7.5 (m, 8H, Ar−H). Anal. Calcd for $C_{61}H_{84}Cl_2O_9$: C. 70.98; H, 8.20; O, 13.95. Found: C, 71.04; H, 8.08; O, 13.82.

Synthesis of Polymers. Poly[[[3-{6-(4′-(2*S*,3*S*)-2-chloro-3-methyl-*n*-pentanoyloxy)-4-biphenyloxy}hexyloxy]-methyl]trimethylene oxide], Polymer-1(6). Compound **3(6)** (2.0 g; 4.0 × 10^{-3} mol) was dissolved in 10 mL of dichloromethane, and to this solution was added boron trifluoride diethyl etherate (0.01 mL; 8.13 × 10^{-3} mmol) under an argon atmosphere. The solution was stirred for 24 h at 0 °C and then poured into 200 mL of methanol. The precipitate thus obtained was filtered. The polymer was purified by reprecipitation into *n*-hexane and methanol. The recovered yield was 1.2 g (60%).

IR (KBr): 3039 (aromatic C−H stretching), 2906 (aliphatic C−H stretching), 1762 (C═O stretching), 1607 and 1482 (aromatic C═C stretchings), 1376, 1206, 1111, and 1035 cm^{-1} (C−O stretchings) and 520 cm^{-1} (C−Cl stretching). ^1H NMR ($CDCl_3$, ppm): δ 0.9−1.85 (m, 19H, $-CH_2-$ and CH_3), 2.23 (m, 1H, −ClCH−*CH*−), 3.25−3.30 (m, 8H, −*CH*$_2$−O−), 3.9 (t, 2H, −*CH*$_2$−OAr), 4.4 (d, 2H, Cl−*CH*−), 6.90, 7.12, 7.43, and 7.50 (d, 8H, Ar−H). Anal. Calcd for $C_{29}H_{39}ClO_5$: C, 69.24; H, 7.81; O, 15.90. Found: C, 69.31; H, 7.79; O, 16.00.

Poly[[[3-{10-(4′-(2*S*,3*S*)-2-chloro-3-methyl-*n*-pentanoyloxy)-4-biphenyloxy}decyloxy]methyl]trimethylene oxide], Polymer-1(10). The recovered yield was 0.75 g (50%).

IR (KBr): 3043 (aromatic C−H stretching), 2907 (aliphatic C−H stretching), 1762 (C═O stretching), 1608 and 1480 (aromatic C═C stretchings), 1374, 1234, and 1115 (C−O stretchings), and 520 cm^{-1} (C−Cl stretching). ^1H NMR ($CDCl_3$, ppm): δ 0.90−1.80 (m, 27H, $-CH_2-$ and CH_3), 2.20 (m, 1H, −ClCH−*CH*−), 3.20−3.40 (m, 8H, −*CH*$_2$−O−), 3.98 (t, 2H, −*CH*$_2$−OAr), 4.40 (d, 2H, Cl−*CH*−), 6.95, 7.15, 7.47, and 7.56 (d, 8H, Ar−H). Anal. Calcd for $C_{33}H_{47}ClO_5$: C, 70.88; H, 8.47; O, 14.31. Found: C, 70.80; H, 8.44; O, 14.28.

Poly[[3,3′-bis[[6-{4′-{(2*S*,3*S*)-2-chloro-3-methyl-*n*-pentanoyloxy}-4-biphenyloxy}hexyloxy]methyl]trimethylene oxide], Polymer-2(6). Compound **10(6)** (2.0 g; 4.0 × 10^{-3} mol) was dissolved in 10 mL of dichloromethane, and to this solution was added boron trifluoride diethyl etherate (0.01 mL;

Scheme 2. Synthetic Route to Monomers for Polymer-2(*n*)

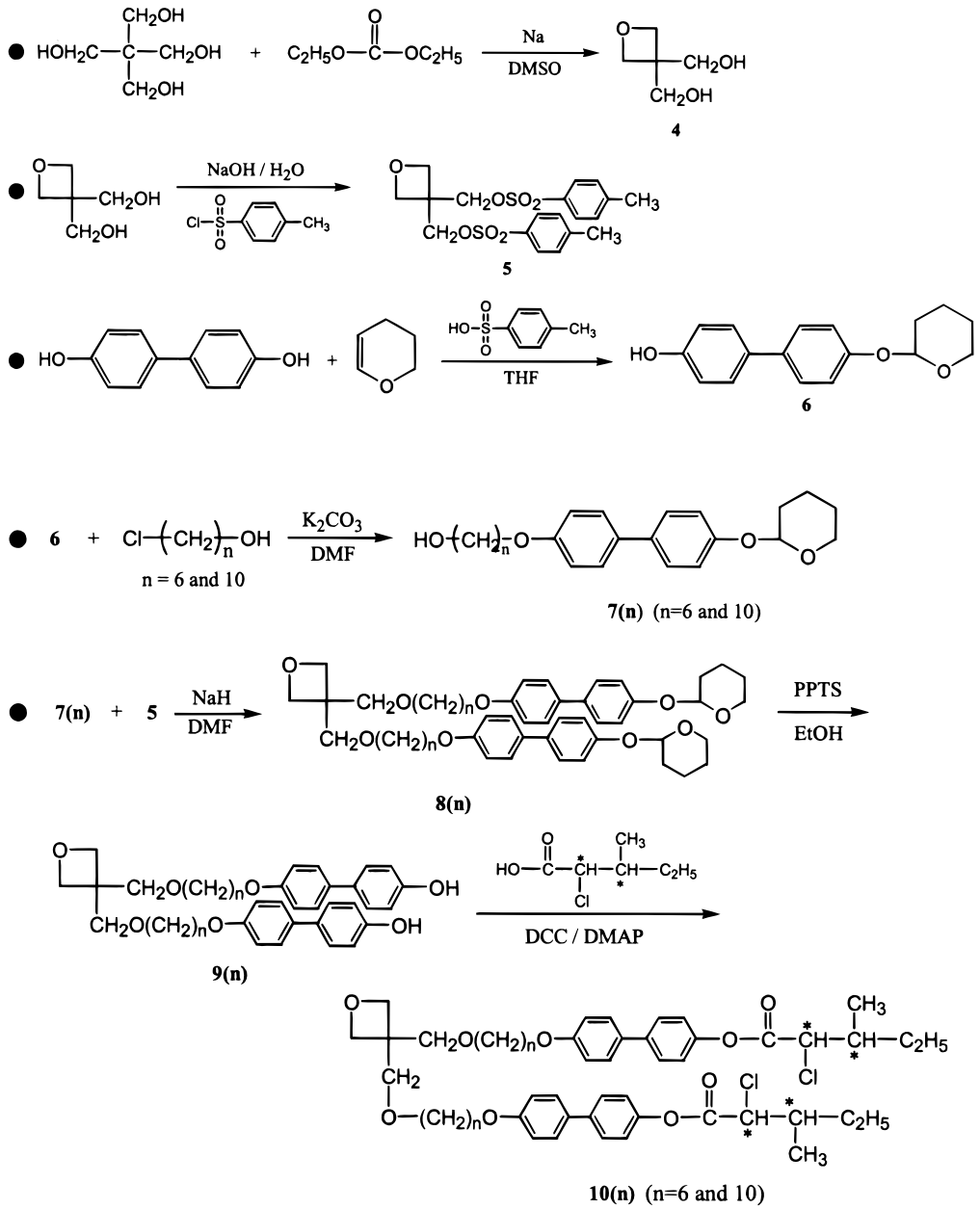

8.13 × 10^{-3} mmol) under an argon atmosphere. The solution was stirred for 72 h at 0 °C and then poured into 200 mL of methanol. The precipitate thus formed was filtered. The polymer was purified by column chromatography on a silica gel column using dichloromethane as an eluent. The conversion was 96%, but the recovered yield was only 0.28 g (21%).

IR (KBr): 2906 (aliphatic C−H stretching), 1764 (C═O stretching), 1607 and 1497 (aromatic C═C stretchings), and 1290, 1206, and 1112 (C−O stretchings), and 515 cm^{-1} (C−Cl stretching). ^{1}H NMR ($CDCl_3$, ppm): δ 0.90−1.85 (m, 32H, $-CH_2-$ and CH_3), 2.23 (m, 2H, −ClCH−*CH*−), 3.25−3.45 (m, 12H, $-CH_2-$O−), 3.9 (t, 4H, $-CH_2-$OAr), 4.4 (d, 2H, Cl−*CH*−), 6.90, 7.10, 7.40, and 7.50 (d, 16H, Ar−H). Anal. Calcd for $C_{53}H_{68}Cl_2O_9$: C, 69.19; H, 7.45; O, 15.65. Found: C, 69.24; H, 7.40; O, 15.69.

Poly[[3,3′-bis[[10-{4′-{(2*S*,3*S*)-2-chloro-3-methyl-*n*-pentanoyloxy}-4-biphenyloxy}decyloxy]methyl]trimethylene oxide], Polymer-2(10). The conversion was 91%, but the recovered yield after purification by chromatography was 0.1 g (20%).

IR (KBr): 2926 (aliphatic C−H stretching), 1763 (C═O stretching), 1607 and 1496 (aromatic C═C stretchings), and 1378, 1249, and 1113 (C−O stretchings), and 515 cm^{-1} (C−Cl stretching). ^{1}H NMR ($CDCl_3$, ppm): δ 0.90−1.90 (m, 48H, $-CH_2-$ and CH_3), 2.20 (m, 2H, −ClCH−*CH*−), 3.20−3.50 (m, 12H, $-CH_2-$O−), 3.95 (t, 4H, $-CH_2-$OAr), 4.40 (d, 2H, Cl−*CH*−), 6.90, 7.10, 7.47, and 7.56 (d, 16H, Ar−H). Anal. Calcd for $C_{61}H_{84}Cl_2O_9$: C, 70.98, H 8.20, O 13.95. Found: C, 70.11; H, 8.34; O, 13.36.

Characterization. The infrared and ^{1}H NMR spectra were recorded on a Bomem MB-series FT-IR instrument and on a Bruker AM 300 NMR spectrometer. Elemental analyses were performed using an Eager 200 elemental analyzer by the Organic Research Institute of Sogang University, Seoul, Korea. Thermal properties of the compounds were examined on a differential scanning calorimeter (Mettler DSC 821^e) at heating and cooling rate of 10 °C/min under a nitrogen atmosphere. Indium was employed as a standard material for calibration of temperature and heat of transition. The glass transition temperature was defined as the temperature where the initial change in slope of the DSC curve occurred, whereas the maximum point in the endothermic peak was taken as the phase transition temperature. Thermal transitions and optical textures of the compounds were also observed through a polarizing microscope (Olympus BH-2) equipped with a hot stage (Mettler FP-82 HT) controlled automatically by the

Scheme 3. Synthetic Route to Polymer-1(*n*) and Polymer-2(*n*)

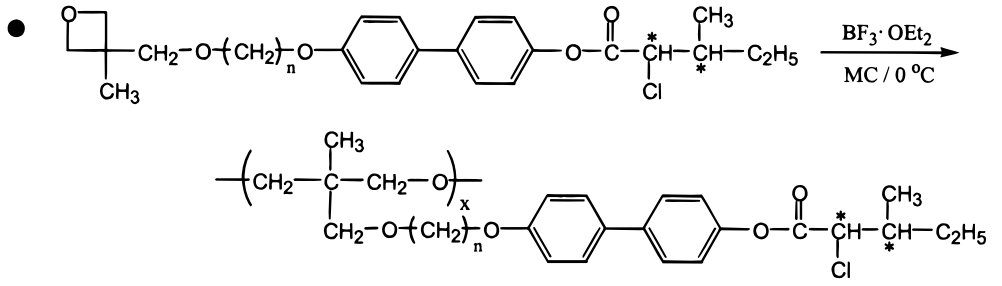

Polymer-1(n) (n=6 and 10)

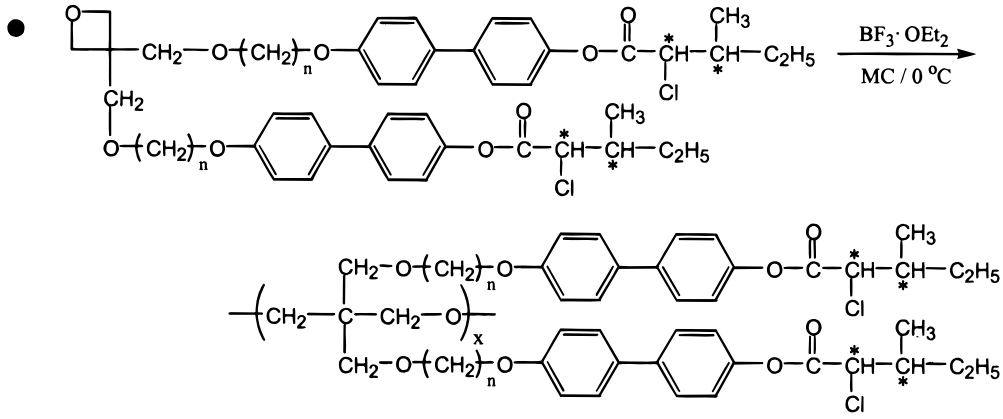

Polymer-2(n) (n=6 and 10)

Table 1. Polymerization Results

polymer	initiator, mol %	monomer concn, mol/L	convn,[a] %	yield, %	$\bar{M}_n$[b]	$\bar{M}_w$[b]	$\bar{M}_w/\bar{M}_n$	$\overline{DP}$[b]
Polymer-1(6)	2	1.0	61	52	21300	55900	2.62	31
Polymer-1(10)	2	1.0	55	50	13600	23600	1.73	24
Polymer-2(6)	2	1.0	96	21	4700	5100	1.09	5.1
Polymer-2(10)	1	1.0	91	20	3700	4500	1.21	3.6

[a] The values were determined by ^{1}H NMR spectroscopy. [b] The values were obtained from GPC.

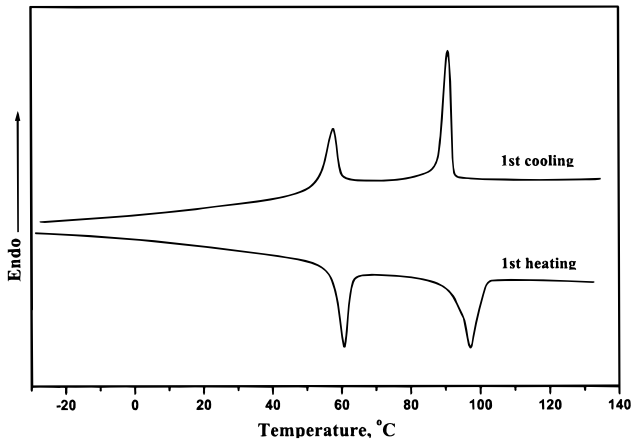

Figure 1. DSC thermograms of **Polymer-1(6)** obtained under a nitrogen atmosphere at the heating and cooling rates of 10 °C/min.

Mettler FP-90 central unit. X-ray diffractograms were obtained on a Rigaku Denki instrument using Ni-filtered Cu Kα radiation (0.1542 nm). The sample holder was heated with two cartridge heaters and temperature was monitored by a thermocouple. Molecular weight was determined using a Waters 150 CV PLUS gel permeation chromatograph.

Results and Discussion

Synthesis of Monomers. All of the intermediates and monomers were synthesized following the synthetic routes shown in Schemes 1 and 2.

Compound **1(*n*)** was synthesized via a two-phase reaction consisting of an aqueous layer of 3-methyl-3-oxetanemethanol and an organic layer of dibromoalkane dissolved in *n*-hexane. Tetrabutylammonium bromide was utilized as a phase transfer catalyst. A large excess dibromoalkane was used in order to reduce the formation of disubstituted side-products. Compound **1(*n*)** and 4,4′-biphenol were condensed in ethanol in the presence of potassium hydroxide. Compound **2(*n*)** thus prepared is not soluble in the aqueous sodium carbonate solution, but 4,4′-biphenol is soluble in the basic solution. Therefore, we could remove unreacted biphenol according to the difference in solubility. The monomer **3(*n*)** was prepared by reacting compound **2(*n*)** with (2*S*,3*S*)-2-chloro-3-pentanoic acid in the presence of 4-(*N*,*N*-dimethylamino)pyridine (DMAP) and *N*,*N*-dicyclohexylcarbodiimide (DCC) as a condensing agent[32] for the esterification reaction.

The monomers **10(*n*)** were prepared via different synthetic procedures. One of the hydroxy groups of 4,4′-biphenol was protected by the tetrahydropyranyl group,

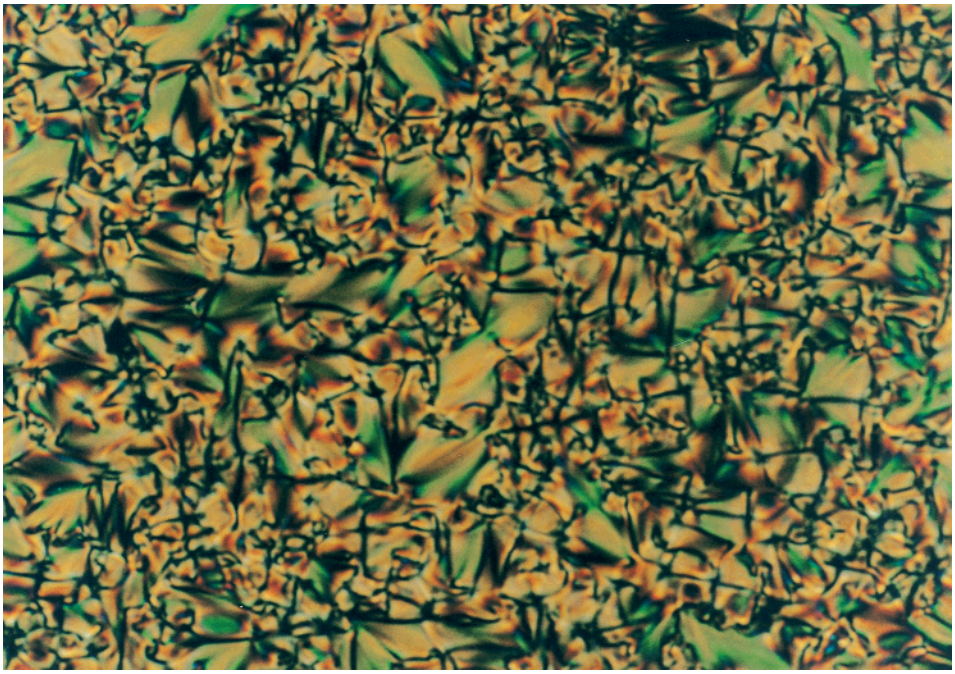

Figure 2. Optical photomicrograph of **Polymer-1(6)** polymer taken at 89 °C (magnification 400×).

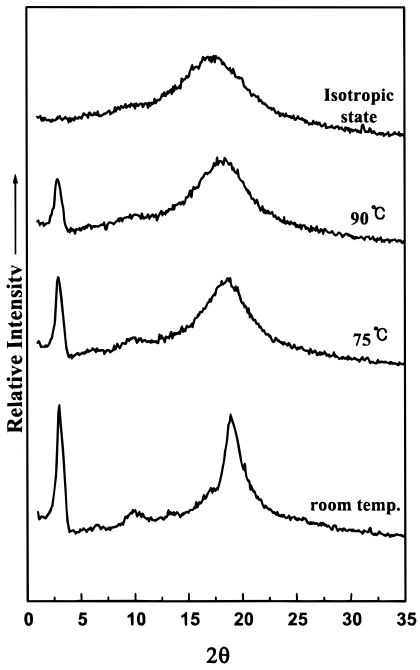

Figure 3. Temperature-dependent wide-angle diffractograms of **Polymer-1(6)** obtained in the cooling cycle. The bottom diffractogram is the virgin polymer sample's diffraction pattern.

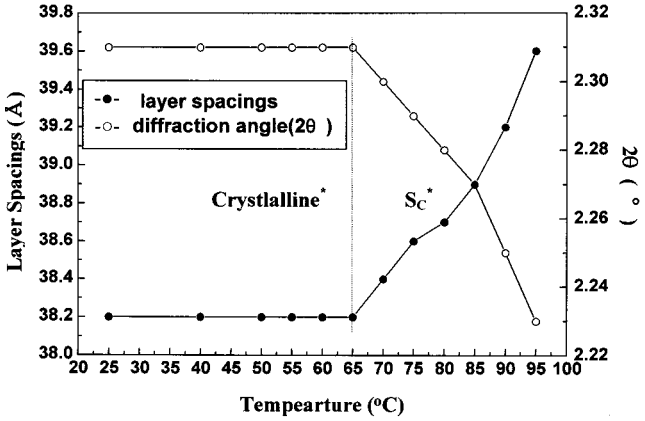

Figure 4. Plot of temperature-dependent layer spacings and diffraction angles for **Polymer-1(6)**.

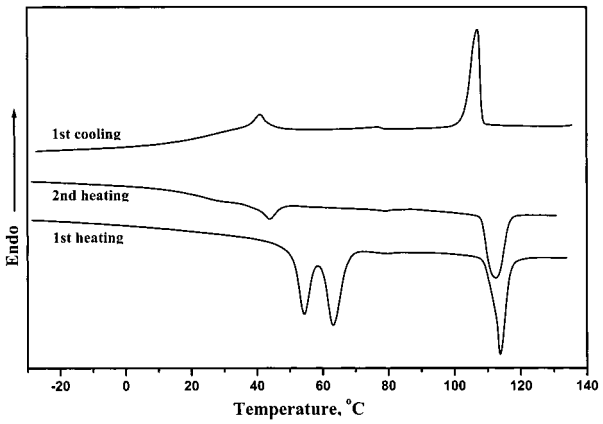

Figure 5. DSC thermograms of **Polymer-1(10)** obtained under a nitrogen atmosphere at heating and cooling rates of 10 °C/min.

and then compounds **7(*n*)** were prepared by reacting the protected biphenol with 6- or 10-chloroalkan-1-ol in DMF using potassium carbonate as a base. Compounds **7(*n*)** and **5** were condensed in DMF in the presence of sodium hydride. The tetrahydropyranyl group in compound **8(*n*)** was removed using pyridinium *p*-toluenesulfonate (PPTS) in ethanol at 55 °C.[33] The oxetane ring was not affected during the above deprotection reaction. Compounds **9(*n*)** were reacted with (2*S*,3*S*)-2-chloro-3-pentanoic acid in the presence of DCC and DMAP resulting in the final monomers. The structures of all the intermediates and the final compounds were confirmed by elemental analyses and IR and NMR spectroscopy. According to the previous report by Hsu et al.,[31] oxetane monomers bearing mesogenic units showed liquid crystalline properties in their melts. We, however, did not find any liquid crystallinity in the monomers **3(6)** and **3(10)**, whereas the monomers **10(6)** and **10(10)** formed monotropic liquid crystal phases. Monomers **10(6)** and **10(10)** formed a smectic mesophase at 46 and

(a)

(b)

Figure 6. Optical photomicrograph of **Polymer-1(10)** taken at (a) 95 and (b) 75 °C (magnification 400×).

59.5 °C, respectively, during the cooling process. We, however, did not carry any further study to identify the nature of their smectic phases.

Syntheses of Polymers. The synthetic routes to the polymers are shown in Scheme 3. The present polymers were synthesized via cationic ring-opening polymerization of oxetane monomers using boron trifluoride diethyl etherate as an initiator. The polymerization reaction was conducted in dichloromethane at 0 °C and the initiator used was 2 mol % of the monomers. For the synthesis of **Polymer-2(10)**, 1 mol % of initiator was utilized. **Polymer-1(6)** and **-1(10)** were purified by reprecipitation into *n*-hexane and methanol several times and obtained as white powders. On the contrary, **Polymer-2*n*** samples were purified by column chromatography after a reprecipitation process. The purity and chemical structures of both types of the polymers were confirmed by IR and ^{1}H NMR spectroscopy. We could determine the conversion (Table 1) based on the area of the resonance peaks corresponding to the protons in

the oxetane ring in ^{1}H NMR spectra of the reaction mixture. The molecular weights (Table 1) of **Polymer-1(6) and -1(10)** were fairly high, $\bar{M}_n$ = 21 300 and 13 600, respectively. Those of **Polymer-2(6)** and **Polymer-2(10)**, however, were relatively low despite longer polymerization times. Their average degrees of polymerization ($\overline{DP}$) were only 5.1 for **Polymer-2(6)** and 3.6 for **Polymer-2(10)**. Analogues of the present polymers, as shown below, were synthesized and characterized earlier by Kawakami et al.[30] They also obtained only low molecular weight oligomers with $\overline{DP}$ being in the range 3−5. This is presumably due to the steric effect of the intermediate propagating species. In other words, the reaction sites near the carbon bearing two large mesogenic units probably make the oxetane monomers difficult to access.

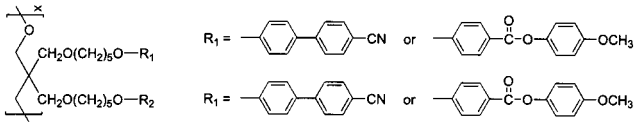

Thermal and Liquid Crystalline Properties. Polymer-1(6) and Polymer-1(10). The thermal and phase transition behaviors of **Polymer-1*n*** were studied by DSC. Figure 1 shows DSC thermograms of **Polymer-1(6)**. They reveal two clear, reversible, phase transition peaks in the heating and cooling cycles. On the first heating curve of DSC runs, a large peak corresponding to the crystal-to-mesophase transition, i.e., melting temperature (T_m) was observed at 61 °C. At a higher temperature another endothermic peak, corresponding to the mesophase-to-isotropic phase transition, was observed at 98 °C. The first cooling cycle of DSC run also exhibits two phase transition peaks at 58 and 90 °C. Only one fluid smectic phase was observed for **Polymer-1(6)** on a polarizing microscope in the first heating cycle, and this smectic phase changed to a crystalline phase on cooling. The texture (Figure 2) of the smectic phase of **Polymer-1(6)** was not developed well despite prolonged annealing at the corresponding temperatures, and, therefore, we could not identify this mesophase by optical texture analysis.

However, the temperature dependent wide- and small-angle X-ray diffractometry strongly indicates that this polymer forms a chiral smectic C (S_C*) phase in its melts. The wide-angle X-ray diffractograms (Figure 3) taken at 75 and 90 °C show rather diffuse peaks in the wide-angle region, corresponding to short-range intermolecular spacings, which implies a fluid LC phase. In addition, they show a sharp peak in the small-angle region corresponding to the long-range order. However, the X-ray diffraction scan taken at room temperature on the cooling cycle seems to be quite different when compared with two diffractograms taken at 75 and 90 °C as shown in Figure 3. The half width of the diffraction peak centered around 2θ = 18.5° (d = 4.8 Å) becomes narrower and it has a small shoulder at 2θ = 17.0° (d = 5.2 Å). Furthermore, the diffraction peak in the small angle region increased in intensity with decreased half-width. It is reasonable to believe that the phase formed below 65 °C should be a crystalline phase which is confirmed by wide-angle X-ray diffractometry. This shape of the diffraction, however, is very similar to that of the diffraction which was assigned as the S_J* phase, as reported by Vallerien et al.[34] We studied wide-angle X-ray diffractograms of **Polymer-1(6)** at room temperature after various thermal treatments. We, however, could not find any significant change in the diffraction patterns after thermal treatments when compared with that of as-polymerized sample. This result suggests that the thermally treated samples may have the same morphology as that of the virgin polymer which is in a crystalline state. A plot of temperature-dependent layer spacings and diffraction angle (2θ) in the small-angle region for this polymer is shown in Figure 4. The long-range spacings evaluated from the small-angle X-ray diffractograms are in range of 38.2−39.6 Å depending on the temperature. As shown in Figure 4, the peak maxima were gradually shifted from 2θ = 2.23 (39.6 Å) to 2θ = 2.31° (38.2 Å) as the temperature was decreased from 95 to 65 °C. In other words, the layer spacing decreased with decreasing temperature. This observation appears to be a general phenomenon in the case of S_C* phases having a helical molecular arrangement.[35,36] However, further decreasing of the layer spacing was not observed.

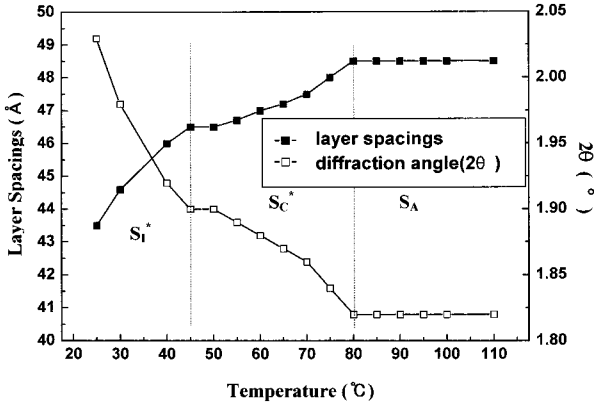

Figure 7. Plot of temperature-dependent layer spacings and diffraction angles for **Polymer-1(10)**.

Figure 5 shows DSC thermograms of **Polymer-1(10)**. Three large endothermic peaks are observed in the first heating curve. We believe that the two peaks at 54 and 63 °C are due to a polymorphic crystal structures of the polymer. When the polymer was annealed at 50 °C, the lower temperature endotherm at 54 °C shifted toward the higher temperature peak. The endothermic peak at 114 °C corresponds to the mesophase-to-isotropic phase transition. This peak was reversible in the heating and cooling curves. A smaller endothermic peak, corresponding to a transition between two different LC phases, was also observed reversibly at 80 °C. However, on the cooling cycle, a transition to a new LC phase was observed around 40 °C instead of a crystallization endotherm. This result was confirmed by texture analysis on a polarizing microscope and by X-ray study.

The optical texture taken at 95 °C exhibits a clear focal conic fan-shaped texture of the smectic A phase (Figure 6a). When the temperature was lowered to 75 °C, the fan-shaped texture (Figure 6b) was a little bit broken, and appearance of the equidistant lines on the surface of the fan, which is the characteristic of the S_C* phase, was observed. The fan shape remained more or less broken below 75 °C, and we did not observe any crystallization.

We examined the temperature dependence of the wide-angle diffraction of **Polymer-1(10).** A remarkable trend observed in the diffraction pattern with decreasing temperature is the fact that the half-width of the diffraction peak in the wide-angle region becomes

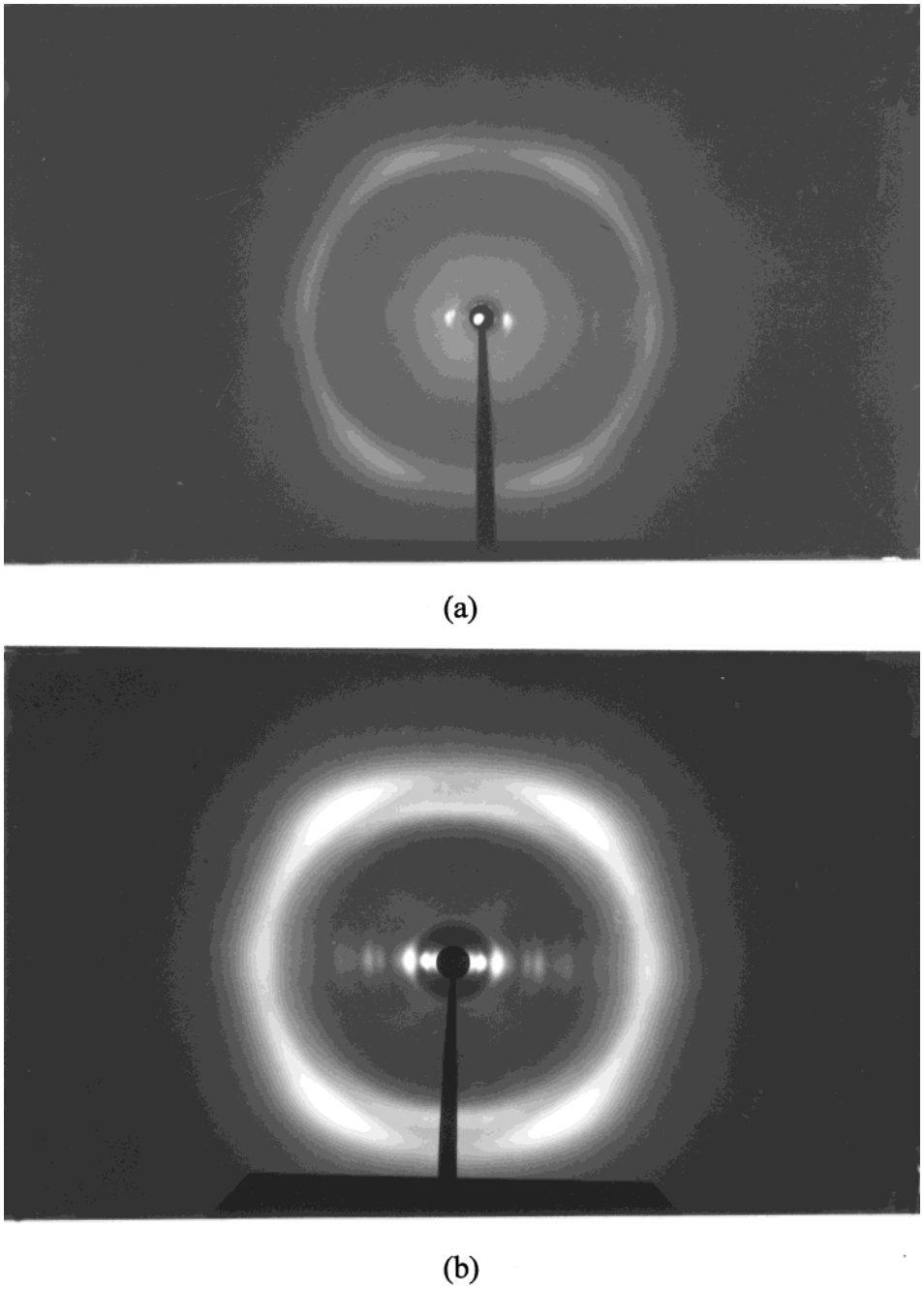

Figure 8. Fiber X-ray diffraction patterns of (a) **Polymer-1(6)** and (b) **Polymer-1(10)**. Fibers were drawn at 90 and 70 °C, respectively. Fiber axis is vertical.

gradually narrower. Besides, the peak maxima corresponding to the interchain distance were slightly moved from $2\theta = 18.9°$ ($d = 4.7$ Å) at 95 °C to $2\theta = 19.3°$ ($d = 4.6$ Å) at room temperature. The satellite small diffraction peaks at $2\theta = 3.63°$ ($d = 24.3$ Å) at 95 °C and $2\theta = 3.70°$ ($d = 23.9$ Å) at 75 °C correspond to possibly the second-order reflections of the first-order ones at $2\theta = 1.82°$ ($d = 48.5$ Å) and $2\theta = 1.86°$ ($d = 47.5$ Å), respectively. On the contrary, the peak at $2\theta = 3.15°$ ($d = 28.1$ Å) on the diffraction scan taken at room temperature deviated from the second-order reflection and was shifted a little more toward the small-angle side. Furthermore, the relative intensity of the peak increased comparatively when compared with that of the peak at $2\theta = 2.02°$ ($d = 43.7$ Å). We did not observed any similar satellite diffraction for **Polymer-1(6)**. The Bragg spacing of 28.1 Å, incidentally, coincides with the length of the smectic monolayer with the tilt angle of 30°. Therefore, it is conjectured that this crystal smectic phase presumably has two kind of layer structures, i.e., monolayer and bilayer. One should note that all the values below $2\theta = 5°$ related on diffraction angles and corresponding Bragg spacings came from small-angle X-ray scans. The reflection in the wide-angle also has a weak shoulder peak centered around at $2\theta = 17°$ ($d = 5.2$ Å) on the left side of the main peak ($2\theta = 19.3°$; $d = 4.6$ Å). However, the diffraction scans of as-polymerized sample as well as two annealed ones show an additional shoulder peak around at $2\theta = 21°$ ($d = 4.2$ Å). This suggests that the annealed or the virgin samples of **Polymer-1(10)** possess a more well-defined lateral arrangement of the molecules within each layer than that of sample which is obtained after cooling from isotropic liquid. On the basis of these X-ray analysis, we deduced that the mesophase formed below 75 °C on cooling is not the crystalline phase but most probably

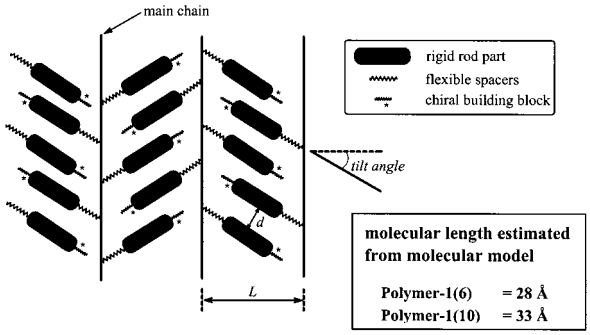

polymer	d (Å)[a]	L (Å)[b]	tilt angle (°)[c]
Polymer-1(6)	4.7 ~ 4.9	38.2 ~ 39.6	30
Polymer-1(10)	4.7	46.2 ~ 48.5	30

[a] Evaluated from WAXD.

[b] Evaluated from SAXD.

[c] Evaluated from fiber X-ray pattern; **Polymer-1(6)** (90 ℃), **Polymer-1(10)** (70℃)

Figure 9. Proposed S_C* phase layer structure of uniaxially oriented **Polymer-1(*n*)**.

the S_I* phase having a helical layers.[35] We could reconfirm the existence of three different types of liquid crystalline phases from the result of the temperature-dependent small-angle X-ray scans of this polymer. Figure 7 describes the relationship between temperature-dependent layer spacings and diffraction angles, which tell us more clearly the helical characteristics of the S_C* and the S_I* phases as well as temperature ranges of the three mesophases.

In addition, the X-ray diffraction patterns of melt-spun fibers of **Polymer-1(6)** and **Polymer-1(10)**, drawn at 90 and 70 °C, respectively, as shown in Figure 8, make us reconfirm that the fluid smectic phases of these polymers have a tilted structure. **Polymer-1(6)** exhibits two pairs of crescent shape reflections in the wide-angle region, centered around $2\theta = 17°$ that correspond to the interchain distance, from which we could evaluate the tilt angle of the mesogenic group being about 30°. And **Polymer-1(6)** exhibits only one pair of equatorial reflections corresponding to the smectic layer spacing in the small-angle region centered around $2\theta = 3°$.

The situation for **Polymer-1(10)**, however, is somewhat different. This polymer shows an additional pair of meridional reflections in the wide angle region as well as two pairs of crescent shape reflections in the wide-angle region centered around $2\theta = 17°$ and one pair of equatorial reflections in the small-angle region centered around $2\theta = 1.8°$. This diffraction pattern is similar to those of the S_G* phase as reported by Zentel et al.[37] They described that unoriented side-chain LC polymers showed the S_C* phase, while oriented samples, i.e., melt-spun fibers, showed the highly ordered S_G* phase according to their X-ray diffraction patterns. We believe that this may be due to the fact that the melt drawing temperature (70 °C) was too low for the smectic phase (S_C*) to be quenched in the same state. However, as we mentioned above, it is more appropriate for the diffraction pattern of **Polymer-1(10)** taken at 70 °C to correspond to the S_I* phase. The tilt angle of the S_C* phase of **Polymer-1(10)** evaluated from the X-ray diffraction pattern is 30°, which is the same as that of **Polymer-1(6)**.

On the basis of these X-ray analyses, we propose that the S_C* mesophases of **Polymer-1(6)** and **Polymer-1(10)** have layered structures as shown in Figure 9. The polymer main chains are packed parallel to each other, and the side mesogenic groups occupy the space between the layer and tilt 30° to the perpendicular axis to the fiber axis. The lamella spacings (d) evaluated from small-angle X-ray diffraction of **Polymer-1(6)** and **Polymer-1(10)** are respectively in the range of 38.2−39.6 and 46.2 ∼ 48.5 Å, depending on the temperature. These values, however, correspond to about 1.4 times an average molecular length (L) of the side groups calculated from CS CHEM 3D assuming fully extended trans conformations for the polymethylene spacers. Therefore, these results imply that the morphology of the smectic phases of the present polymers is that of intercalated bilayer smectic. The value of d/L for the intercalated bilayer smectic phase is well-known to be in the range of 1.3−1.6.[35,38]

Polymer-2(6) and Polymer-2(10). The thermal and liquid crystalline properties of the **Polymer-2*n*** are quite different than those of the previous polymers. First of all, **Polymer-2(6)**, the analogue of **Polymer-1(6)**, did not show liquid crystallinity. As shown in DSC thermograms of **Polymer-2(6)** showed only one large peak at 147 °C corresponding to the crystal-to-isotropic liquid transition. We, also, could not observe any liquid crystalline optical texture on the polarizing microscope. Indeed, temperature-dependent X-ray diffractograms of **Polymer-2(6)** tell us that the polymer does not form any liquid crystal phases. All of the oxetane polymers reported by Kawakami et al.,[30] which have similar length of the polymethylene spacers, exhibit nematic or smectic phases, although the chemical structures of their mesogenic units are different from that of the present **Polymer-2(6)**. The situation for **Polymer-2(10)**, however, is completely different. The DSC thermograms of **Polymer-2(10)** show two exothermic peaks on the cooling cycle and three endothermic peaks on the heating cycle. We believe that the first two endothermic peaks on the heating curve at 114 and 119 °C come from the polycrystalline morphology of the polymer, because the lowest temperature peak is shifted toward to and merged with the higher temperature peak when the polymer was annealed at 110 °C. The endotherm at 128 °C corresponds to the transition of the mesophase-to-isotropic phase. The large exothermic peak at 128 °C on the cooling curve corresponds to the isotropic liquid-to-liquid crystal phase transition, and the small one at 102 °C corresponds to the mesophase-to-mesophase transition. We conducted optical polarizing microscopy at a considerably slow cooling rate (0.3 °C/min) in order to observe a well-developed optical textures of mesophases. The higher temperature liquid crystalline phase started to be formed at 132 °C and remained to 102 °C. It must be noted that the above-mentioned cooling rate is so slow that one cannot closely correlate the optical observation results with those DSC especially in absolute values of transition temperatures. The optical texture (Figure 10a) of the polymer taken at 120 °C exhibits a smectic fan texture. As the observation temperature was reduced below 102 °C, a broken-fan texture was developed (Figure 10b) and preserved to room temperature. The X-ray diffraction scan taken at 125 °C in the process of cooling (0.3 °C/min) shows a broad diffraction in the wide-angle region centered around $2\theta = 17°$, which corresponds to the interchain distance (4.2 Å) and implies a fluid LC phase. The reflection at $2\theta = 5.5°$ ($d = 16.1$ Å) tells us that this fluid LC phase is a smectic. Although we could not

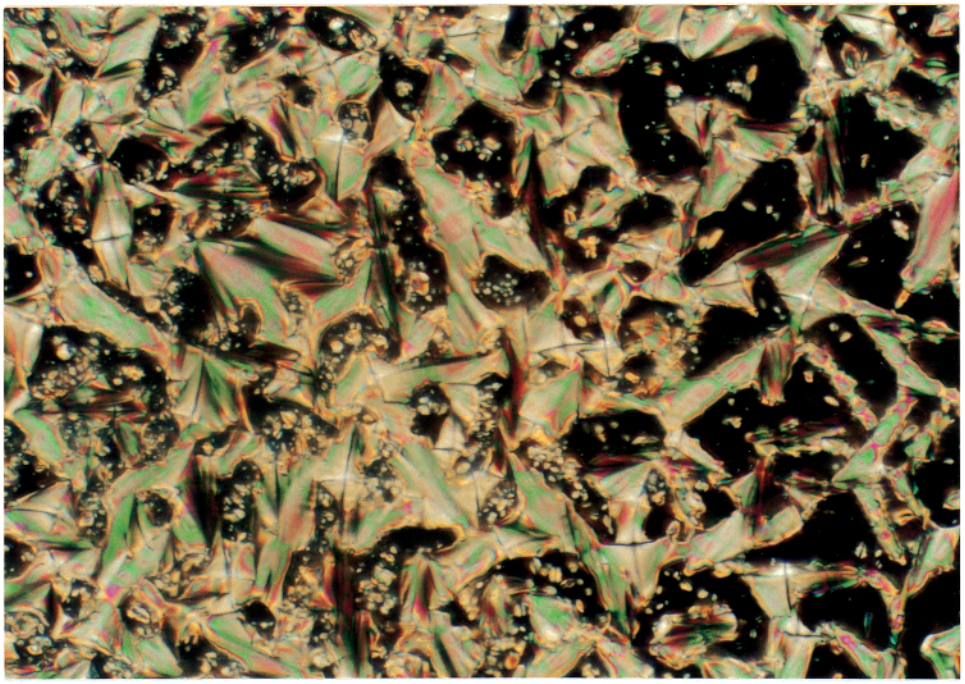

(a)

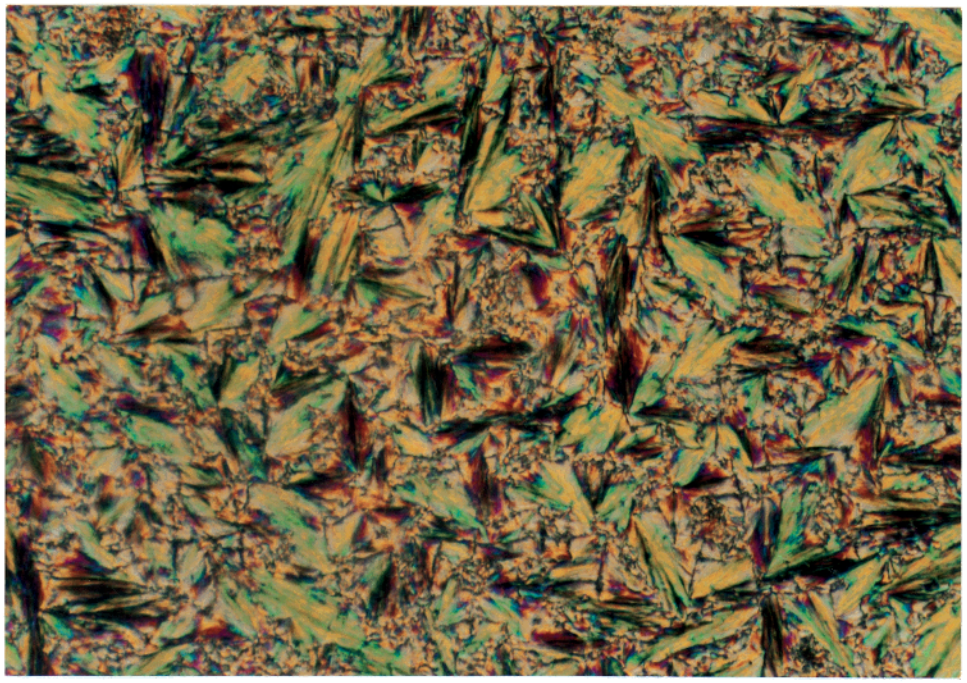

(b)

Figure 10. Optical photomicrograph of **Polymer-2(10)** taken at (a) 120 °C and (b) room temperature (magnification 400×).

define exactly the identity of the higher temperature mesophase, it is supposed to be a S_C* phase based not only on the fact that the phase has a fluidity but also on the fact that the color of the optical textures depended on temperature. The diffraction peaks at $2\theta = 1.8°$, $2\theta = 3.4°$, and $2\theta = 5.2°$ on the X-ray diffractogram of this polymer obtained at room temperature, which correspond to spacings of 49.1, 26.0, and 17.0 Å, respectively, confirm that this polymer has a layered structure in its mesophase. The diffraction peak in the wide-angle region split into two, one at $2\theta = 17.6°$ ($d = 5.0$ Å) and the other at $2\theta = 20.0°$ (4.4 Å), which implies that the lower temperature mesophase of **Polymer-2(10)** could be an S_I* phase.

Electrooptical Properties. The ferroelectric properties on of **Polymer-1(6)** and **Polymer-1(10)** in the S_C* phase were investigated by the triangular wave method.[3,23,24,39] The polymers were placed between two ITO-coated glass plates whose surface were coated with polyimide and then rubbed.[40] A weak optical bistability

could be observed on a polarizing microscope while a electric field was applied across a 1.8 μm thick sample. However, we could not measure the values of spontaneous polarization (P_s) regardless of a variation in electric field (5−50 V) and frequency (1−60 Hz). This result may be attributed to a high melt viscosity in the S_C* phase, and partially to an imperfect alignment of mesogens.

In general, the P_s values decrease as the melt viscosity increases, and very often it cannot be measured when the melt viscosity is very high.[19,22,41] And the alignment quality of the sample also has an effect on the P_s value.[22,42] Another important point to be noted is that the proposed S_C* phase layer structure shown in Figure 9 implies the formation of antiferroelectric mesophase by these polymers. This possibility has to be further studied.

Conclusion

We synthesized new side-chain liquid crystalline polyoxetanes by cationic ring-opening polymerization. **Polymer-2(6)** and **Polymer-2(10)** having the same two side chain mesogens in the repeating unit were obtained only in considerably low molecular weight. On the contrary, the molecular weights of **Polymer-1*n*** ($n = 6$ and 10), were reasonably high. The monomers, **3(*n*)**, for **Polymer-1*n*** carries only one pendant mesogenic group. It is clear that the presence of two bulky pendant mesogens in the monomers **10(*n*)** exert a strong steric hindrance in polymerization. All of the present polymers except **Polymer-2(6)** exhibited liquid crystalline phases such as S_A, S_C*, and S_I* phases in their melts. As one can expect, the polymers with a longer spacer length (**Polymer-1(10)** and **Polymer-2(10)**) exhibited a higher variety in liquid crystalline phases over a more broad temperature range. In particular, we propose that the smectic phases of the present polymers have intercalated bilayer structure. We were not successful in obtaining the values of spontaneous polarization (P_s), although a weak optical bistability could be observed for the S_C* phases. There also a possibility that some of the polymers form an antiferroelectric phase.

Acknowledgment. The research was supported by the Korea Science and Engineering Foundation through the Center for Electro- and Photo-Responsive Molecules, Korea University.

Supporting Information Available: Text giving details of the syntheses of the monomers used in this paper. This material is available free of charge via the Internet at http://pubs.acs.org.

References and Notes

(1) Meyer, R. B.; Liebert, L.; Strzelecki, L.; Keller, P. *J. Phys.* **1975**, *36*, P69.
(2) Poths, H.; Wischerhoff, E.; Zentel, R.; Schönfeld, A.; Henn, G.; Kremer, F. *Liq. Cryst.* **1995**, *18*, 811.
(3) *Ferroelectric Liquid Crystals−Principles, Properties and Appication*; Goodby, J. W. G., et al., Eds.; Gordon and Breach Science: Philadelphia, PA, 1991.
(4) Lu, R. B.; Xu, K. H.; Lu, Z. H. *Liq. Cryst.* **1999**, *26*, 553.
(5) Jakli, A.; Müller, M.; Krüerke, D.; Heppke, G. *Liq. Cryst.* **1998**, *24*, 467.
(6) Goodby, J. W.; Leslie, T. M. *Mol. Cryst. Liq. Cryst.* **1984**, *110*, 175.
(7) Arakwa, S.; Matsui, E.; Nito, K.; Yasuda, A. *Liq. Cryst.* **1997**, *23*, 659.
(8) Clark, N. A.; Lagerwall, S. T. *Appl. Phys. Lett.* **1980**, *36*, 1.
(9) Fukuda, A.; Ouchi, Y.; Arai, H.; Takano, H.; Ishikawa, K.; Takezoe, H. *Liq. Cryst.* **1989**, *5*, 1055.
(10) Leister, N.; Geschke, D. *Liq. Cryst.* **1998**, *24*, 441.
(11) Shilov, S.; Gebhard, E.; Skupin, H.; Zentel, R.; Kremer, F. *Macromolecules* **1999**, *32*, 1570.
(12) Mitsuishi, M.; Ito, S.; Yamamoto, M.; Endo, H.; Hachiya, S.; Fischer, T.; Knoll, W. *Macromolecules* **1998**, *31*, 1565.
(13) Cooray, N. F.; Fujimoto, H.; Kakimoto, M.; Imai, Y. *Macromolecules* **1997**, *30*, 3169.
(14) Ruth, J.; Naciri, J.; Shashidhar, R. *Liq. Cryst.* **1994**, *16*, 883.
(15) Poths, H.; Schönfeld, A.; Zentel, R.; Kremer, F.; Siemensmeyer, K. *Adv. Mater.* **1992**, *4*, 351.
(16) Scherowski, G.; Beer, A.; Coles, H. J. *Liq. Cryst.* **1991**, *10*, 809.
(17) Suzuki, T.; Okawa, T. *Makromol. Chem., Rapid Commun.* **1988**, *9*, 755.
(18) Shibaev, V. P.; Kozlovsky, M. V.; Beresnev, L. A.; Blinov, L. M.; Platé, N. A. *Polym. Bull.* **1984**, *12*, 299.
(19) Scherowski, G.; Fichina, U.; Wolff, D. *Liq. Cryst.* **1995**, *19*, 621.
(20) Sekiya, T.; Yuasa, K.; Uchida, S.; Hachiya, S.; Hashimoto, K.; Kawasaki, K. *Liq. Cryst.* **1993**, *14*, 1255.
(21) Omenat, A.; Hikmet, R. A. M.; Lub, J.; Sluis, P. *Macromolecules* **1996**, *29*, 6730.
(22) Dumon, M.; Nguyen, H. T.; Mauzac, M.; Destrade, C.; Gasparoux, H. *Liq. Cryst.* **1991**, *10*, 475.
(23) Naciri, J.; Pfeiffer, S.; Shashidhar, R. *Liq. Cryst.* **1991**, *10*, 585.
(24) Helgee, B.; Hjertberg, T.; Skarp, K.; Andersson, G.; Gouda, F. *Liq. Cryst.* **1995**, *18*, 871.
(25) Shibaev, V. P.; Kozlovsky, M. V.; Platé, N. A.; Beresnev, L. A.; Blinov, L. M. *Liq. Cryst.* **1990**, *8*, 545.
(26) Kawakami, Y.; Takahashi, K.; Hibino, H. *Macromolecules* **1991**, *24*, 4531.
(27) Kawakami, Y.; Takahashi, K.; Nishiguchi, S.; Toida, K. *Polym. Int.* **1993**, *31*, 35.
(28) Motori, M.; Noguchi, K.; Arano, A.; Kanoh, S.; Ueyama, A. *Bull. Chem. Jpn.* **1993**, *66*, 1778.
(29) Lu, Y. H.; Chang, H. L.; Hsu, C. S. *Polym. Bull.* **1994**, *32*, 551.
(30) Kawakami, Y.; Kato, Y. *Polym. J.* **1997**, *29*, 775.
(31) Hsu, L.-L.; Chang, T.-C.; Tsai, W.-L.; Lee, C.-D. *J. Polym. Sci., Part A: Polym. Chem.* **1997**, *35*, 2843.
(32) Doleschall, L. *Tetrahedron Lett.* **1963**, 1195.
(33) Miyashita, M.; Yoshikoshi, A.; Grieco, P. A. *J. Org. Chem.* **1977**, *42*, 3772.
(34) Vallerien, S. U.; Zentel, R.; Kremer, F.; Kapitza, H.; Fischer, E. W. *Makromol. Chem., Rapid Commun.* **1989**, *10*, 333.
(35) *Smectic Liquid Crystals−Textures and Structures*; Gray, G. W.; Goodby, J. W. G., Eds.; Leonard Hill: Glasgow, Scotland, 1984.
(36) Cooray, N. F.; Kakimoto, M.; Imai, Y.; Suzuki, Y. *Polym. J.* **1993**, *25*, 863.
(37) Zentel, R.; Reckert, G.; Reck, B. *Liq. Cryst.* **1987**, *2*, 83.
(38) Barny, P. L.; Dubois, J.-C.; Friedrich, C.; Noël, C. *Polym. Bull.* **1986**, *15*, 341.
(39) Scherowsky, G. *Ferroelectric Polymers*; Nalwa, H. S., Ed.; Marcel Dekker: New York, 1995; Chapter 10.
(40) Hall, A. W.; Lacey, D.; Hill, J. S.; Blackwood, K. M.; Jones, M.; McDonnell, D. G.; Sage, I. C. *Liq. Cryst.* **1996**, *20*, 437.
(41) Scherowsky, G.; Müller, U.; Springer, J.; Trapp, W.; Levelut, A. M.; Davidson, P. *Liq. Cryst.* **1989**, *5*, 1297.
(42) Méry, S. J.; Nicoud, J.-F.; Guillon, D. *Macromolecules* **1995**, *28*, 5440.

MA000346U